Inorganic Chemistry
Article
Cite This: Inorg. Chem. XXXX, XXX, XXX−XXX
pubs.acs.org/IC

Studies of Redox Cofactor Pyrroloquinoline Quinone and Its Interaction with Lanthanides(III) and Calcium(II)

Henning Lumpe and Lena J. Daumann*

Department of Chemistry, Ludwig-Maximilians-Universität München, Butenandtstr. 5-13, 81377 Munich, Germany

Supporting Information

ABSTRACT: Recently it was discovered that lanthanides are biologically relevant and found at the centers of many bacterial proteins. Poorly understood, however, is the evolutionary advantage that certain lanthanides might have over calcium at the center of methanol dehydrogenase enzymes bearing redox cofactor PQQ. Here, we present a straightforward method to obtaining clean PQQ from vitamin capsules. Furthermore, we provide full NMR, IR, and UV−vis spectroscopic characterizations of PQQ. We conducted NMR experiments with the stepwise addition of diamagnetic and paramagnetic lanthanides to evaluate the binding to PQQ in solution. This study provides a deeper understanding of PQQ chemistry and its interaction with lanthanides.

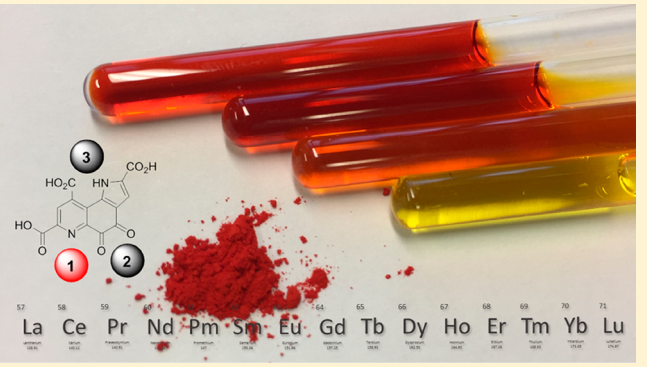

INTRODUCTION

Oxidoreductases are a group of enzymes which transfer redox equivalents from or to substrates.[1] While nicotinamide or flavin are commonly found cofactors in such enzymes,[2] in 1964 Anthony and Zatman discovered an enzyme with an alternative, noncovalently bound redox cofactor,[3] which was later determined to be pyrroloquinoline quinone (PQQ, methoxatin). PQQ-containing enzymes form the oxidoreductase subgroup of quinoproteins and are an essential part of the energy metabolism of many organisms.[2]

Redox cofactor PQQ is activated by a Lewis acid.[5] For more than 30 years, it was thought that calcium was the only metal ion that had this function in nature. However, many methanol-oxidizing bacteria can in fact produce two types of MDH: the traditional one that has been studied intensively for more than 50 years uses calcium, and a second one, which has only recently been discovered, uses lanthanides instead of calcium. Lanthanides have long been thought to have no biological relevance but are now firmly established as the natural metal ion cofactors in MDH enzymes that are encoded by the *xoxF* gene.[4,6] Phylogenetic analysis shows that this lanthanide-dependent class of MDH is, in fact, more widespread in nature and might be evolutionarily older than its calcium counterpart and perhaps the major pathway for methanol oxidation in methylotrophic bacteria growing on methane or methanol.[7] The first structure of a Ln-MDH was obtained from the XoxF-MDH isolated from strain *Methylacidiphilum fumariolicum* SolV and was reported by Pol et al.[4] The active site (Figure 1) contains a nine-coordinate lanthanide ion, surrounded by cofactor PQQ, three carboxyl groups from Asp_{299}, Asp_{301} (a residue that is lacking in Ca-MDH), and Glu_{172} as well as an amide from Asn_{256}. This MDH X-ray structure was refined

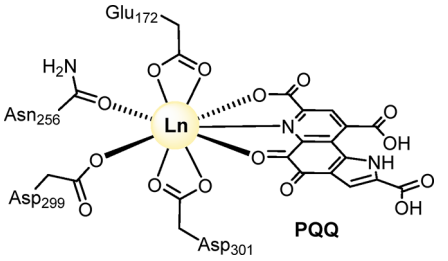

Figure 1. Active site visualization of Ln-MDH from strain SolV, including cofactor PQQ, central metal Ln, and surrounding amino acid residues.[4]

with Ce^{3+}(PDB 4MAE). Structures of a Eu-MDH (PDB 6FKW) from the same organism and a La-MDH (PDB 6DAM) from *Methylomicrobium buryatense* 5GB1C are now also available, showing similar active site arrangements.[8] In Ca-MDH, PQQ is coordinated in the same way by the Lewis acid (Site 1, Figure 2).[9] Many bacteria possess genes for both MDH enzymes encoded by *mxaF* (Ca-MDH) and *xoxF* (Ln-MDH) and can switch between them depending on Ln availability; this has been termed the "lanthanide switch".[10] It has been shown that *Methylorubrum extorquens* AM1 preferentially expresses Ln-MDH even with only nanomolar concentrations of lanthanides and a 20 μM concentration of Ca in the cultivation medium.[11] The trivalent lanthanides are better Lewis acids than calcium, and it has been suggested that they pose an advantage in the redox cycling of PQQ.[12] Furthermore, it has been shown that not all lanthanides

Received: February 26, 2019

DOI: 10.1021/acs.inorgchem.9b00568
Inorg. Chem. XXXX, XXX, XXX−XXX

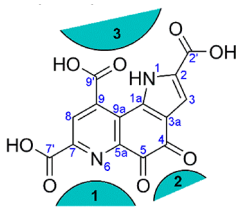

Figure 2. PQQ numbering scheme according to Unkefer et al.[14] and possible binding sites in solution, adapted from Nakamura et al.[15]

promote methanol oxidation in Ln-MDH equally.[4,8a,10d,11b,13] For the native metalloenzyme isolated from SolV, it has been shown that the enzyme functions more efficiently with early lanthanides (La–Nd).[13a] Bacteria also prefer early lanthanides for growth and show improved uptake of these elements.[4,13c] The lanthanide switch, the advantage over calcium, and why some Ln are better than others are currently not yet fully understood.

Cofactor PQQ was first isolated by Anthony and Zatman[16] and was later determined to be a quinone by Duine et al.[17] Salisbury et al.[18] reported the first crystal structure of the acetone adduct and proposed the structure of PQQ, shown in Figure 2. The unusual orthoquinone structure of PQQ, detected in the EPR measurements of Duine et al., led them to propose the name pyrrolo-quinoline quinone for this new prosthetic group.[19] In successive years, PQQ was extensively studied regarding total synthesis,[20] adduct formation with nucleophiles,[21] redox behavior,[22] and metal ion interaction (Ca^{2+})[23] with several reviews published.[2,24] PQQ has also been proposed to be a vitamin for humans; however, these claims remain doubtful.[25] Previously, it was reported that PQQ without the surrounding enzyme pocket is capable of the coordination of metal ions at three positions (Figure 2). This is supported by several crystal structure determinations (site 1[26] (Cu), site 2[27] (Ru), and site 3[15] (Cu)). For Ca^{2+}, no crystal structure exists with PQQ by itself, but studies of trimethylester derivative PQQTME **2** in MeCN suggest a coordination mode similar to that of MDH.[23] In light of the discovery of lanthanide-dependent metalloenzymes, we have investigated the metal ion coordination behavior of PQQ in solution by NMR and UV–vis spectroscopy using lanthanides and calcium. Our studies suggest that in solution the coordination of lanthanides occurs in the same position as in MDH (site 1) and that even if PQQ acts as a tridentate ligand (C_5=O, N_6, C_7–CO_2H) the Ln-PQQ complexes undergo fast exchange in solution. In this study, we have investigated diamagnetic trivalent lanthanides La and Lu as well as calcium(II) and compared them with paramagnetic lanthanides Ce, Pr, Sm, Eu, Tb, Er, and Tm.

EXPERIMENTAL SECTION

Nuclear Magnetic Resonance (NMR). ^{1}H NMR and ^{13}C NMR spectra were recorded, unless otherwise stated, at room temperature or 0 °C with Jeol ECP 270 (400 MHz), Jeol ECX 400 (400 MHz), and Bruker Avance III (400 MHz) spectrometers operating at 400 MHz for proton nuclei and 100 MHz for carbon nuclei. Low-temperature measurements (−50 °C) were performed on a Varian NMR System (400 MHz). ^{1}H chemical shifts are reported in units of ppm relative to DMSO-d_6 (δ_H = 2.50) and DMF-d_7 (δ_H = 8.03). ^{13}C chemical shifts are given in units of ppm relative to DMSO-d_6 (δ_H = central line of septet: δ_C = 39.52) and DMF-d_7 (central line of triplet: δ_C = 163.15). The software used for data processing was MestReNova version 11.0. Two-dimensional heteronuclear multiple quantum correlation (HMQC) and heteronuclear multiple bond connectivity (HMBC) experiments were used to assign each resonance in the spectra. Experiments were performed by default with 16 scans for ^{1}H and 4000 scans for ^{13}C experiments and were increased to up to 64 scans for ^{1}H and 10 000 scans for ^{13}C for correct assignments and side-product analysis. Solid state NMR was performed at room temperature with a Bruker Avance III (500 MHz, 11.74 T) with magic-angle spinning (MAS) in 4 mm rotors. ^{1}H with single pulse excitation, ^{13}C with cross-polarization over ^{1}H. Scan delays (d1): ^{13}C, 16 s; ^{1}H, 128 s. Chemical shifts are reported in units of ppm relative to TMS, indirectly measured with 0.1% TMS in $CDCl_3$. All NMR spectra are included in the Supporting Information.

Stepwise Addition of Lanthanide(III) and Calcium(II) Salts to PQQ. Metal-induced NMR shifts were used to examine the position of coordinating metals to PQQ in solution. PQQ shows good solubility in polar solvents such as H_2O (pH >7), MeOH, DMSO, and DMF but not in MeCN. While metal addition to aqueous solutions of PQQ leads to the precipitation of a 1:1 complex, solutions in methanol give a hemiketal adduct as the predominant species, which complicates analysis. In DMSO, significant solvent complexation can also occur and is comparatively stronger than in other solvents ($[Ln(DMSO)_8]^{3+}$. For a summary, see Cotton and Harrowfield.[28] Therefore, DMF-d_7 was the solvent of choice for coordination experiments. Unless otherwise noted, the NMR tube contained PQQ (9 mg, 27 μmol), which was dissolved by sonication at 50 °C for 5 min. $LiClO_4$ (16 mg, 0.15 mmol) for controlled ionic strength and Ln/Ca salts were always added as solids and were dissolved by sonication at 50 °C for 5 min. In the case of very small amounts of metal (0.01 equiv), a stock solution was prepared in DMF-d_7 (0.01 mg/μL), which was used for metal addition (0.01 equiv equals ∼10 μL of stock solution (Table S1)). ^{1}H and ^{13}C NMR spectra were recorded within 1 h after the metal addition. Experiments with larger amounts of PQQ (50 mg, 151 μmol) in DMF-d_7 (0.6 mL) were performed in the same way, but higher temperatures (65 °C) were necessary to ensure complete dissolution. All NMR experiment conditions can be found in Table S1, and shifts can be found in Tables S2–S4. **FT-infrared spectroscopy (IR)** was carried out with a Jasco FT/IR-460 Plus with an ATR diamond plate. IR data can be found in Table S5 and Figures S3 and S4. **UV–vis spectroscopy** of the different PQQ derivatives was conducted with an Agilent 8453 diode array spectrophotometer in a 1-cm-path-length quartz Suprasil cuvette. The following stock solutions were prepared: PQQ in DMF or DMSO (4 mM). A blank was recorded with 990 μL of solvent (DMF/DMSO/H_2O), followed by the addition of 10 μL of the respective PQQ stock solution (4 mM) to yield a final concentration of 4 μM. For measurements in H_2O, the PQQ stock solution in DMF was used, leading to a total DMF concentration of 1% in the cuvette. Spectra were recorded instantly after mixing. UV–vis spectra can be found in Figure S5. UV–vis spectroscopy of PQQ (**1**) in DMF or water with lanthanide chloride and calcium chloride was performed on an Epoch 2 plate reader from Biotek using a 96-well quartz microplate from Hellma. In DMF, measurements included 190 μL of a PQQ stock solution in DMF (42.1 μM) and 10 μL of DMF or 10 μL of $LnCl_3{\cdot}nH_2O$ (Ln = La–Lu, n = 7 for La–Ce and n = 6 for Pr–Lu, except for Sm and Dy, where n = 0) or $CaCl_2{\cdot}2H_2O$ in DMF (0.8 mM) to yield a final concentration of 40 μM for both PQQ and the metal salts (1:1) (Figure 6). In a subsequent experiment, 2 μL of DMF and 2 μL of $LnCl_3{\cdot}nH_2O$ (Ln = La–Lu, except Pm) or $CaCl_2{\cdot}2H_2O$ in DMF (40 mM) were added to the respective well, resulting in a final PQQ concentration of 39.6 μM and a PQQ to metal ratio of 1:11. A blank was recorded in pure DMF (200 μL), and the resulting absorbance was subtracted from the spectra. Additional UV–vis spectra can be found in Figures S10 and S11. Measurements in water included 180 μL of a PQQ stock solution in H_2O (278 μM), 20 μL of H_2O or 18 μL of H_2O, and 2 μL of $LnCl_3{\cdot}nH_2O$ (Ln = La–Lu, n = 7 for La–Ce and n = 6 for Pr–Lu, except Sm and Dy, where n = 0) or $CaCl_2{\cdot}2H_2O$ in H_2O (25 mM) to yield a final concentration of 250 μM for both PQQ and metal salts (1:1) (Figure S7). A solvent blank was recorded and subtracted from the respective spectrum. Job's plot measurements included PQQ as well as $LuCl_3$ (anhydrous)

DOI: 10.1021/acs.inorgchem.9b00568
Inorg. Chem. XXXX, XXX, XXX–XXX

stock solutions in DMF (200 μM, Figure S9) or in water (250 μM, Figure S8) and were conducted using a plate reader (Epoch 2). For the PQQ stock solution in water, a concentrated DMF solution was prepared first (25 mM), which was diluted with water to the final 250 μM concentration (including 130 mM DMF). The $LuCl_3$ stock solution in water was treated with the same amount of DMF (130 mM). Both water- and DMF-based measurements included x μL of PQQ + y μL of $LuCl_3$ (x = 200, 190, 180, ..., 0) ($y = 200 - x$), a total of 20 different ratios. For data processing, the corrected extinction of PQQ was calculated at 343 nm (data analysis in water) or 435 nm (in DMF) and plotted against the mole fraction of added lutetium(III). The stepwise addition (0.2 equiv steps) of metal salts to a fixed concentration of dissolved PQQ included stock solutions of PQQ (333.33 μM) in water and a 5 mM stock solutions of $LaCl_3{\cdot}7H_2O$, $LuCl_3{\cdot}6H_2O$, or $CaCl_2{\cdot}2H_2O$ in water. Each well contained 200 μL total volume, including 150 μL of PQQ + x μL of metal salt + y μL of water (x = 0, 2, 4, ..., 50) ($y = 50 - x$), resulting in 250 μM PQQ with increasing amounts of metal salts (0.2 equiv per 2 μL added) (Figures 5 and S6).

Elemental Microanalyses (EA). (C, H, N) were analyzed with a vario EL element analyzer. Inductively coupled plasma optical emission spectroscopy (ICP-OES) was conducted with a Varian-Vista instrument with autosampler and was used for determining lanthanide and calcium contents in precipitates. Samples were digested in hot nitric acid and then diluted with Millipore water to a final HNO_3 concentration of 3%. The following wavelengths (nm) were used for metal content determination: La (333.749, 408.671), Eu (381.967, 397.197), Lu (291.139), and Ca (393.366, 396.847). The values shown are averaged. **DFT calculations** were performed with *Gaussian 09*, revision D.01.[29] All calculations were performed using the B3LYP functional,[30] and the 6-31g(d) basis set was used. Solvent effects were modeled using the conductor-like polarizable continuum model (CPCM) with the default setting for the universal force field (UFF).[31] Magnetic properties (NMR shifts) were calculated by the gauge-independent atomic orbital (GIAO) method.[32] Calculated structures and shifts can be found in Table S6. **Thermogravimetric analysis (TGA)** was performed on a TGA 4000 system from PerkinElmer using Al_2O_3 crucibles, and the plots can be found in Figure S13. ESI mass spectra of PQQ were recorded with a Thermo Finnigan LTQ FT ultra Fourier transform ion cyclotron resonance mass spectrometer with acetonitrile/water as the carrier solvent.

Materials. Metal salts were purchased from abcr Germany ($LnCl_3{\cdot}nH_2O$-Ln, 99.9% = Nd, Sm, Gd, Tb, Dy, Ho, Er, Tm, Yb, Lu; $Ln(NO_3)_3{\cdot}nH_2O$-Ln, 99.99% = La, Lu), Sigma-Aldrich ($LnCl_3{\cdot}nH_2O$-Ln, 99.99% = La, Ce, Pr, Eu), Alfa Aesar ($LiClO_4$, 99%; $Ca(NO_3)_3{\cdot}4H_2O$, 99.9995%), and VWR ($CaCl_2{\cdot}2H_2O$, 99%). The water of crystallization of the lanthanides (nH_2O) was analyzed by elemental microanalysis prior to experiments and is given in the respective experimental descriptions. Deuterated solvents were purchased from Sigma-Aldrich (DMF-d_7, 99.5%) and EurIsotop (DMSO-d_6, 99.8%). PQQ was either used from a commercial source (Fluorochem Ltd. Hadfield, 97% purity. (EA) Found: C, 47.81; H, 3.02; N, 7.98. Calcd for $[C_{14}H_6N_2O_8{\cdot}1.4H_2O]$: C, 47.31; H, 2.5; N, 7.88) or conveniently (and cheaply) extracted from Doctor's Best Science-Based Nutrition PQQ capsules, as described below, and transferred from its disodium salt to the fully protonated form, which gave PQQ in high purity. Milli-Q-grade water (pH 5.5), received from a Millipore Synergy UV system from Merck (Darmstadt, Germany), was used for all experiments.

Isolation and Purification of PQQ. PQQ was extracted from Doctor's Best Science-Based Nutrition BioPQQ capsules containing PQQ (as PQQ disodium salt), cellulose, and modified cellulose. The capsules (60 × 20 mg of PQQ = 1.20 g, 3.21 mmol) were emptied, and the powder was suspended in water (250 mL). While the PQQ sodium salt was soluble in water, the cellulose which remained as a solid was filtered off and washed several times with water until the filtrate was colorless. The water was subsequently removed from the filtrate under reduced pressure to give the disodium salt of PQQ as a brown powder (1.12 g, 2.99 mmol, 93%). ^{1}H NMR (400 MHz, DMSO-d_6): δ/ppm = 8.61 (s, 1H, 8), 7.08 (d, J = 1.4 Hz, 1H, 3). IR (neat): $\tilde{\nu}/cm^{-1}$ = 3303, 2360, 2171, 1668, 1603, 1541, 1499, 1339, 1230, 905, 712. EA: Found C 35.72; H 3.39; N 5.93. Calcd for $C_{14}H_4N_2Na_2O_8{\cdot}5.5H_2O$ (PQQ disodium salt) (373.98): C 35.53; H 3.19; N 5.92. The isolated $PQQNa_2$ was converted to the fully protonated form according to a literature procedure.[33] In brief, crude $PQQNa_2$ (1.12 g, 2.99 mmol) was dissolved in water (500 mL) and heated to 70 °C. Concentrated HCl (2.3 mL) was added, and the mixture was stirred at 70 °C for 24 h. The resulting precipitate was filtered, washed with 2 M HCl, and dried in vacuo. The product (1.02 g, 3.09 mmol, 91%) was isolated as a bright red solid. Total yield over two purification steps: 85%. IR (neat): $\tilde{\nu}/cm^{-1}$ = 1742 (m), 1699 (m), 1640 (s) (C═O); 1506 (m) (C═N); 1191 (s), 1263 (s), 1315 (s) (C═C); 865 (m) (C−N). EA: Found: C, 48.04; H, 2.50; N, 7.93. Calcd for $[C_{14}H_6N_2O_8{\cdot}\ 1.15\ H_2O]$: C, 47.92; H, 2.38; N, 7.98. HRMS (ESI− , H_2O/MeCN): m/z calcd for $[C_{14}H_5N_2O_8]^-$: 329.0051; found: 329.0051.

PQQ-Metal Complex Precipitation from Water. $PQQNa_2$ (30 mg, 0.08 mmol as received from Doctor's Best PQQ capsules) was dissolved in H_2O (12 mL). $LaCl_3{\cdot}7H_2O$ (A: 0.5 equiv, 14.9 mg, 0.04 mmol/B: 1.0 equiv, 29.8 mg, 0.08 mmol/C: 2.0 equiv, 59.5 mg, 0.16 mmol) was added as a solid, resulting in immediate turbidity and a color change from dark red to light brown. The suspension was centrifuged (5 min at 4500 rpm in a Heraeus Megafuge 8R benchtop centrifuge with a swinging bucket), and the colorless supernatant was removed. To wash the resulting pellet, water was added (12 mL), and the suspension was first vortex mixed and then centrifuged (same configuration), followed by the removal of the supernatant. This washing step was repeated two more times. The pellet was then transferred to a Schlenk flask and dried overnight under high vacuum to afford A: 26 mg, B: 23 mg, and C: 43 mg of a brown powder. EA (CHNLa): (A) Found C, 30.42; H, 2.44; N, 5.17; La, 25.94. (B) Found: C, 31.21; H, 2.34; N, 5.22; La 22.97. (C) Found: C, 30.14; H, 2.50; N, 5.19; La 25.18. Calcd for PQQLa·5H_2O $[C_{14}H_{13}LaN_2O_{13}]$: C, 30.23; H, 2.36; N, 5.04; La, 24.98. The experiments were repeated with $CaCl_2{\cdot}2H_2O$ (0.5, 1.0, 2.0, and 3.0 equiv), $EuCl_3{\cdot}6H_2O$ (1.0 and 3.0 equiv), and $LuCl_3{\cdot}6H_2O$ (1.0 and 3.0 equiv), each indicating a PQQ·M·5H_2O complex as well. (IR data are available in the Supporting Information, Figure S5.) We have attempted to obtain mass spectra of the M-PQQ complexes; however, we mostly observed PQQ (**1**) and the geminal diol (**3**, Figure S1).

RESULTS AND DISCUSSION

Study of PQQ Metal Ion Interactions in Water. After precipitation of PQQ the water equivalent present in the solid could not be removed by drying at 100 °C or under high vacuum. To exclude the possibility that the solid could be the water adduct of PQQ (**3**, a geminal diol can result from the hydration of the quinone **1** at the C5 position, Figures 2 and 3) solid state NMR was performed, which indicated pure PQQ (**1**) and can be found in the Supporting Information (Figure S2A). IR spectra of disodium salt and purified fully protonated PQQ can be found in the Supporting Information (Figure S3, Table S5). The solubility of PQQ in water is limited to its (partially) deprotonated form (pK_a = 0.30 (N_6), 1.60 (C_7-CO_2H), 2.20 (C_9-CO_2H), 3.30 (C_2-CO_2H), 10.30 (N_1)).[34] In addition, PQQ will form the geminal diol (**3**) in a molar ratio of 2(**1**):1(**3**) in water, as observed with NMR by Duine et al.[35] In DMF, PQQ will form **3** to some extent when traces of water are present or introduced by the addition of metal salts containing waters of crystallization (Figure S1A). On the basis of DFT calculations (Table S6), we propose that this addition is taking place at the C5 carbon. The formation of a diol is evidenced by a new resonance at 91.7 ppm stemming from a diol moiety in position 5. The formation of **3** is also supported by ESI mass spectrometry in a H_2O/MeCN mixture where both PQQ (**1**, m/z = 329.0051, $[C_{14}H_5N_2O_8]^-$) and PQQ-

DOI: 10.1021/acs.inorgchem.9b00568
Inorg. Chem. XXXX, XXX, XXX−XXX

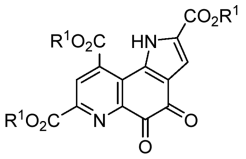

R^1=H (**1**, PQQ)
R^1=Me (**2**, PQQTME)

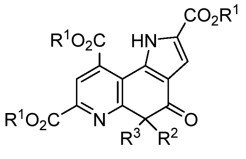

R^1=H, R^2=OH, R^3=OH (**3**, PQQ-H_2O)
R^1=Me, R^2=OH, R^3=OH (**4**, PQQTME-H_2O)
R^1=H, R^2=OMe, R^3=OH (**5**, PQQ hemiketal)
R^1=Me, R^2=OMe, R^3=OH (**6**, PQQTME hemiketal)

Figure 3. Structures of the different PQQ species and PQQ adducts referred to in this study.

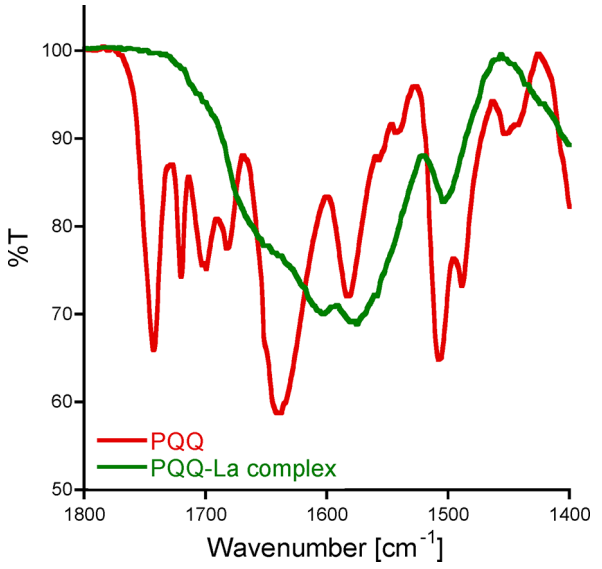

Figure 4. Overlayed IR spectra of PQQ (red) and the PQQ-La complex (green) between 1800 and 1400 cm^{-1}.

H_2O (**3**, m/z = 347.0157 [$C_{14}H_7N_2O_9$]$^-$) are observed (Figure S1B). Previously, Zheng and Bruice also showed with calculations that (methanol) adducts at C5 of PQQ are energetically favored.[36] When trivalent lanthanide ions or calcium(II) were added to an aqueous, concentrated solution of $PQQNa_2$ (pH >7), a 1:1 PQQ–metal complex precipitated. Elemental microanalysis of the solids revealed similar stoichiometries, regardless of the amount of added metal salt. Analysis suggested the formation of a PQQ·M·5H_2O complex (M = Ca^{2+}, La^{3+}, Eu^{3+}, Lu^{3+}), although the exact coordination mode in the solid state could not be ascertained. TGA analysis of the solids (PQQ + Eu or La) did not give a clear indication of whether the five water molecules were bound tightly to the metal ion in the complex or were present as cocrystallized water molecules or whether one of them was covalently bound to PQQ to form **3**. TGA analysis showed a continuous weight loss to 84% on heating to 100 °C, which fits with the elimination of the five water molecules (Figure S13). The compound then gradually lost three CO_2 molecules until it was heated to 500 °C (Figure S13). Numerous attempts to recrystallize the solid or obtain single crystals suitable for X-ray crystallography were unsuccessful. IR spectra of solid PQQ showed seven bands between 1743 and 1583 cm^{-1} which can be attributed to the C=O stretching vibrations of the carboxyl and quinone groups (Figure 4).[37]

A complex of PQQ with Ti^{4+} in binding site 1, previously described by Dimitrijevic et al,.[38] led to a splitting of the quinone signal into two features (1643 to 1653 and 1636 cm^{-1}) and an intensity reduction of one of the carbonyl stretches (1744 cm^{-1}) due to coordination to C_5=O and C_7–CO_2H while the other carbonyl signals remained unaffected. It is important to note that the affected carboxyl group was denoted by Dimitrijevic et al.[38] to be an ester, stemming from an impurity in their PQQ sample. However, their PQQ data match that obtained in the present work (from biological synthesis and fermentation, a highly purified sample), making the previous ester assignment doubtful and the feature at 1744 cm^{-1} more likely to be a carboxylic acid stretch. In our study, the coordination with lanthanum(III) led to a strong shift of all seven carboxyl and quinone absorption bands and the appearance of a broad, poorly resolved feature between 1734 and 1521 cm^{-1}(Figure 4). In the IR spectra of Fe^{2+} and Fe^{3+} complexes with structural PQQ analogues, the bands associated with the coordinated carboxyl groups (C_7) are much more strongly shifted, or disappear completely, in comparison to noncoordinating carboxyl or ester groups (C_9).[39] Hence, a clear statement about the coordination mode of lanthanides solely by IR data remains difficult, but the data indicate a participation of all three carboxyl groups in a three-dimensional coordination network in the solid state with different coordination modes.

An analysis of the PQQ-lanthanide complexes in water was difficult because the precipitation of Ln-PQQ complexes limited the investigations to UV–vis spectroscopy at low concentrations. Furthermore, as mentioned above, PQQ forms at least two species (**1** and **3**) in aqueous solution. Upon metal ion addition, there are then at least four different species present: **1**, **3**, and M-1, and M-3. The UV–vis spectra of PQQ with the stepwise addition of lanthanum(III) or lutetium(III) in unbuffered water is shown in Figure 5. Both lanthanides induce a decrease in the 330 and 478 nm transitions of PQQ (mixture of **1** and **3**) and give rise to an additional absorption feature at 375 (La) or 380 (Lu) nm, respectively. With the same amount of calcium(II), the changes are less pronounced and the new feature is not as red-shifted and appears at 357 nm. The absence of clear isosbestic points and overlapping transitions and the presence of more than two species complicates the analysis of the stoichiometry in solution using Job's method (Figure S8).[40]

Study of PQQ Metal Ion Interactions in Nonaqueous Solvents. The coordination chemistry of PQQ was previously examined with several transition metals as well as sodium ions in both the solid state and in solution. Depending on the metal and the coligands, all three possible binding sites of PQQ can be occupied: With structural PQQ analogues (benzoquinolines) and Fe^{2+},[39] or with C9-decarboxy PQQ and Cd^{2+},[41] or with Cu^{2+},[41] coordination was observed in site 1 (Figure 1). With Cu^{2+}, PQQ and 2,2′-bipyridine (bipy) or terpyridine (terpy) coordination also took place in site 1,[42] as well as with Cu^{2+}, PQQ and terpy,[15] and with Cu^+, PQQTME and PPh_3 as coligands also in site 1.[26] With Cu^+, PQQ and terpy,

DOI: 10.1021/acs.inorgchem.9b00568
Inorg. Chem. XXXX, XXX, XXX–XXX

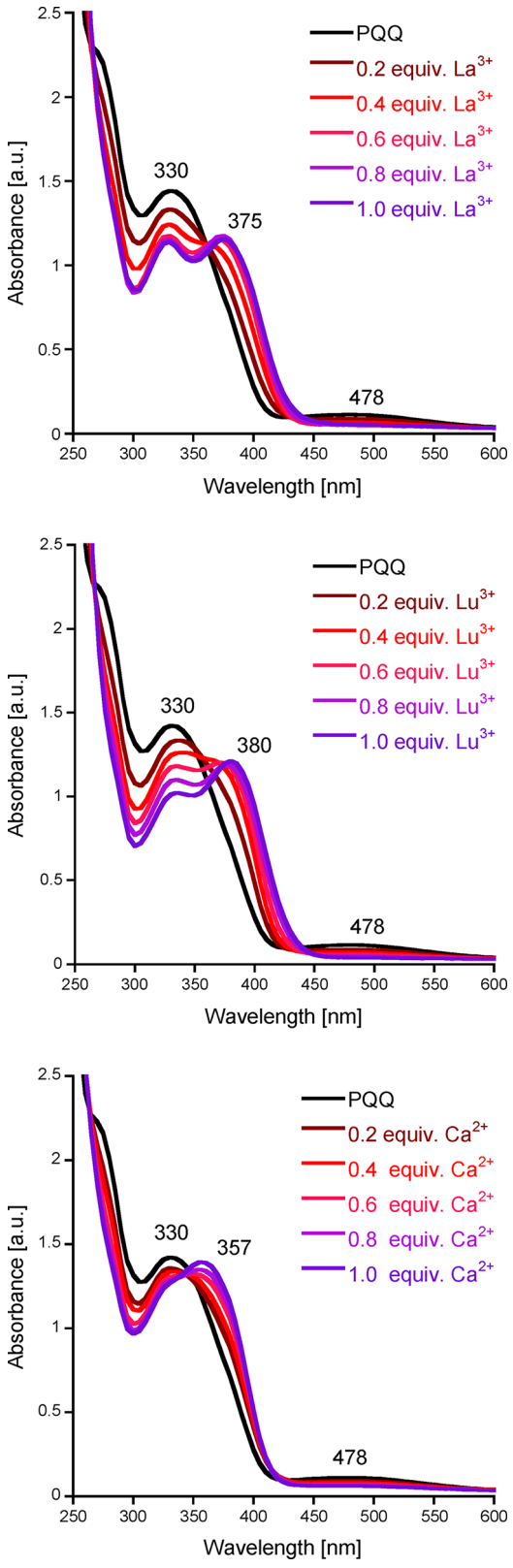

Figure 5. UV−vis spectra of PQQ in H_2O (250 μM) with increasing equivalents of $LnCl_3{\cdot}nH_2O$ (Ln = La, Lu) or $CaCl_2{\cdot}2H_2O$, directly measured after metal addition. For spectra of the complete Ln series and data showing the addition of up to five metal equivalents, see Figures S6 and S7.

coordination took place in sites 1 and 3,[43] and with Ru^{2+}, PQQ and bipy in site 2.[44] With Na^+, coordination was observed in all three sites.[45]

Itoh et al. described a Ca^{2+} coordination with trimethyl ester PQQTME (**2**) in MeCN solution, where shifts of the proton and carbon NMR resonances indicated coordination in site 1.[23,46] However, not all PQQ signals were mentioned, and no indication was given of the PQQ/metal ratio. An ESI mass spectrometry, UV−vis spectroscopy, and in silico study of the interaction of the uranyl ion and Ca^{2+} with PQQ suggested binding in site 1.[47] In 2018, Schelter described a La^{3+} coordination in site 1 with an MDH active site model ligand containing a structural PQQ analogue (benzoquinoline quinone).[48] Here, we examine the interaction of PQQ (**1**) with lanthanides for the first time directly, without the help of structural analogues or methylester species PQQTME (**2**). As mentioned above, water proved to be problematic for metal coordination experiments as a result of the precipitation of a poorly soluble complex at higher concentrations, limiting the analysis in water to UV−vis spectroscopy. PQQ shows good solubility in MeOH, DMF, and DMSO and for the $PQQNa_2$ salt also in H_2O (UV−vis spectra are included in the SI, Figure S5 and Table S7). Because PQQ is known to form hemiketal adducts in methanol (**5**, **6**),[35a] and water adducts (to yield **3**), additional coordination experiments were conducted in DMF. UV−vis experiments with a stepwise addition of lanthanides and calcium ions to PQQ are shown in Figures 6 and S9−S11.

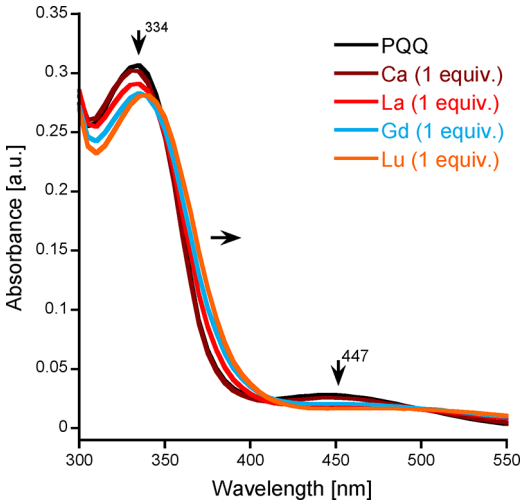

Figure 6. UV−vis spectra of PQQ in DMF (40 μM) with 1 equiv of $LnCl_3{\cdot}nH_2O$ (Ln = La, Gd, Lu) or $CaCl_2{\cdot}2H_2O$, measured directly after metal addition. For spectra of the complete Ln series, see Figure S10.

The UV−vis spectrum of PQQ (**1**) in DMF is only slightly influenced by Ca^{2+}, leading to a decrease in the intraligand absorption bands at 334 and 447 nm. Throughout the lanthanide series, the absorption intensity is steadily reduced upon addition of 1 equiv of Ln (La^{3+} to Gd^{3+}), accompanied by a small but steady shift toward longer wavelengths. The effects of metal ions on PQQ in DMF are much weaker than in water. However, coordination to Ln in DMF clearly influences the electronic structure of PQQ. From Tb^{3+} onward, the red shift is more pronounced, with the maximum absorbance now being at 340 nm. However, the intensity change of the absorption (upon Tb^{3+} to Lu^{3+} addition) is less drastic as with the earlier

DOI: 10.1021/acs.inorgchem.9b00568
Inorg. Chem. XXXX, XXX, XXX−XXX

lanthanide-series ions (Figure S10). We can only speculate as to why such a clear break between early and late lanthanides appears, but a decrease in the coordination number, caused by the lanthanide contraction, is common for lanthanide complexes and could also be of relevance here.[49] Kaim et al. had previously observed a shift from 364 and 434 to 378 and 488 nm upon binding of Cu^+ to the trimethylester derivative (**2**) in CH_2Cl_2.[26] Our experiment in DMF shows that the interaction of **1** with Ln follows a pattern that can be attributed to the different properties of the lanthanides (decrease in ionic radii and increase in Lewis acidity) caused by the lanthanide contraction. Spectra were recorded again after 15 min and with a total PQQ/metal ratio of 1:11 (Figures S10 and S11), leading to a further increase in the observed effects: red shift and absorption intensity change. The addition of water (10 μL, 5 vol %) to the DMF solution decreases the intraligand absorption bands even further but causes only a slight red shift (Figure S10 and S11). Because of the up to 7 equiv of water in the lanthanide salts, not only metal coordination but also water-adduct formation has to be taken into account. This is also further elaborated on in the NMR section below. Because lutetium generated the strongest shift in the UV−vis spectrum in DMF, we attempted to analyze the binding of this lanthanide using the method of continuous variation (Job's plot)[50] in the absence (to avoid the formation of **3**) and presence of traces of water.[40] Because the most pronounced change in the absorption spectrum of PQQ, without other overlapping transitions, was in the region of 435 nm, we used this wavelength for our analysis. As mentioned above, PQQ can add water, and thus we have to assume the presence of multiple PQQ species before even adding metal ions. We thus collected the data in dry DMF and with anhydrous $LuCl_3$. The data collected directly after mixing PQQ with Lu^{3+} suggest a PQQ/Lu 1:1 complex (mole fraction ∼0.5, Figure S9). Surprisingly, the absorbance changed slightly over time (within 15 min), shifting the maximum of Job's plot to 0.6, which could indicate a different stoichiometry and/or the presence of a dynamic process/formation of another species. We want to emphasize here that the complex nature of multiple species of PQQ in solution clearly hampers a straightforward analysis of stoichiometry in solution and that PQQ does add traces of water at the C5 position, leading to the formation of a water adduct (**3**). When using $LuCl_3{\cdot}6H_2O$ instead of anhydrous lutetium salt, the shift over time was stronger, clearly indicating an effect of water on PQQ. Furthermore, the curvature was stronger in DMF, indicating a low binding affinity of PQQ (Figure S9). We have also explored the possibility of learning about the coordination of lanthanides using the hypersensitive transitions that some Ln exhibit.[51] As can be seen in Figure S12, the hypersensitive transitions of the Nd^{3+} ion are visible before and after PQQ addition. The transition at 578 nm gains some intensity; however, within this experimental setup, no meaningful insight into the nature of the coordination sphere of Nd was obtained. To investigate the site of coordination in solution further, we conducted NMR experiments on **1** with the stepwise addition of different lanthanides. Full NMR data of **1** in DMSO are included in the Supporting Information (Table S4); however, this solvent is known to be more strongly coordinating (to lanthanides)[28] and **1** is less soluble in DMSO, hence DMF was used to investigate the interaction with metal ions. Initial investigations included Ca^{2+} and diamagnetic Ln salts La^{3+} and Lu^{3+}, with chlorides and nitrates as counterions with increasing amounts of added metal salts from 1 to 10 equiv and with and without controlled ionic strength ($LiClO_4$). For all three metals and regardless of the counterion employed, the resulting shift for both ^1H and ^{13}C experiment was very small, with the exception of C_9 (Figure 2, para to N_{pyr}). In addition, new resonances appeared in both ^1H and ^{13}C experiments, especially with increasing amounts of added metals. Because of the presence of up to seven waters of crystallization per added lanthanide equivalent, the formation of a water adduct is plausible. In fact, the addition of water itself (20 equiv, 9.8 μL) to a solution of **1**, $CaCl_2$(10 equiv), and $LiClO_4$ in DMF further increased the intensity of the new signal sets, confirming the presence of the water adduct (**3**). Even a sample of purified **1** showed minute traces of additional signals due to trace amounts of residual water. A recrystallized pure sample of **1**, which contained 2 equiv of DMF crystal solvent but no traces of water, did not show such additional signals in the ^1H NMR recorded in dry DMF (Figure S14). This demonstrates that PQQ readily adds water in nonaqueous solvents even when only minute traces are present, confirming our conclusions from UV−vis spectroscopy. On the basis of DFT NMR-shift calculations, this addition is proposed to take place at the C_5 carbon (Table S6). In contrast to the experiments with PQQTME (**2**) described by Itoh,[23] where one coordination site is blocked (site 3, see Figure 2), a clear conclusion solely based on resonance shifts as to where metal coordination takes place with the diamagnetic metal ions and PQQ (**1**) proved to be challenging. Interestingly, besides the discussed water resonances, no new resonances which could be attributed to complex formation appeared. Thus, temperature-dependent NMR experiments with $La(NO_3)_3$ (0.5 equiv) were conducted at r.t., 0 °C, and −50 °C (the lowest accessible temperature within our experimental setup), but regardless of the temperature, only one signal set was visible for PQQ, suggesting a fast exchange in solution even at low temperatures. However, all resonances were further shifted depending on the temperature (^1H and ^{13}C: $C_{9'}$, $C_{7'}$, $C_{2'}$, and C_{5a} downfield, with all other signals upfield).

Experiments with lanthanides and 2,6-dipicolinic acid (dpa) reported by Piguet and co-workers showed a similar phenomenon:[52] excess ligand, added to an already-formed $[Lu(dpa)_3]$ complex in D_2O, gave distinct NMR signals for free and bound ligands, which merged to one signal set at higher temperatures. Hence, −50 °C is likely not low enough to affect a signal separation in our experiments. While no strong metal-induced shifts could help with the assignment of the coordination position, we recognized a broadening of some resonances with increasing amounts of lanthanum and lutetium but not with calcium. Especially with lutetium, the addition of 1 equiv caused resonances $C_{7'}$, C_7, and C_9 to almost disappear in the noise, and exponential line broadening (6.5 Hz) had to be used to make them visible (Figure 7). To further study the coordination mode of PQQ to biologically relevant metals in solution, paramagnetic lanthanides were used.[53] Shifts of the light paramagnetic Ln-chlorides (Ce, Pr, Sm, Eu) for ^1H experiments with 0.5 equiv of metal salt were expectedly stronger than the ones from diamagnetic Ln (0.04−0.19 (H_1), 0.05−0.62 (H_8), 0.01−0.11 (H_3)), and all signals became broadened, especially the H_8 signal (Eu > Pr > Ce > Sm, Tables S1−S3). With increasing amounts of metal salt (0.5−3.0 equiv), all signals were further shifted and broadened (8 > 1 > 3). Shifts of ^{13}C experiments were in the same range as those from diamagnetic Ln; however, resonances that decreased in intensity or completely disappeared due to strong

DOI: 10.1021/acs.inorgchem.9b00568
Inorg. Chem. XXXX, XXX, XXX−XXX

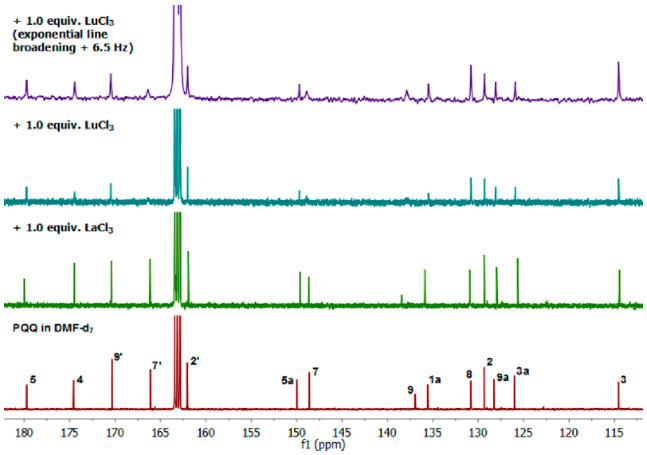

Figure 7. Stacked ^{13}C spectra of **1** in DMF-d_7 (27.2 μmol) with 1.0 equiv of $LaCl_3 \cdot 7H_2O$ or $LuCl_3 \cdot 6H_2O$ showing the broadening of some resonances after the addition of these diamagnetic metal ions.

broadening (especially C_5, $C_{7'}$, and C_7) were induced by lower metal ion concentrations. With 0.5 equiv, certain resonances were already undetectable (Figure 8). With Pr and Eu, more

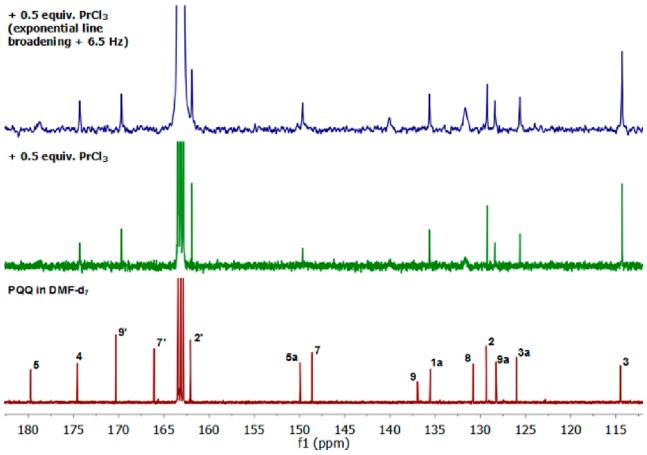

Figure 8. Stacked ^{13}C spectra of **1** in DMF-d_7 (27.2 μmol) with 0.5 equiv of $PrCl_3 \cdot 6H_2O$, showing the disappearance of some resonances after metal addition.

resonances decreased in intensity or disappeared than with Ce and Sm (Table S3), probably stemming from differences in the electronic structure and the magnetic susceptibility tensor of the lanthanides.[53a,c,54] The resonances, which disappeared, were partially different (Table S3) and were affected by the amount of added metal.

The only resonances which remained unaffected in these experiments were C_{1a}, C_{3a}, and C_3. With the heavier, paramagnetic Ln-chlorides of Tb, Er, and Tm, 0.01 equiv of metal salt led to the above-mentioned changes. Because of the commonly known pseudocontact shift of paramagnetic compounds,[53c,55] the spectral width of ^{13}C experiments was increased to −300 to 600 ppm.[52] However, no additional resonances were detected in this range. It is still possible that, because of the paramagnetically induced broadening, the resonances were indeed shifted to low field or high field but were too broad to be observed. Experiments were also repeated with larger amounts of PQQ (50 mg, 143.2 μmol) with 1 equiv of $CeCl_3$ or $PrCl_3$, but besides the now clearly visible resonances of the water adduct (**3**), no additional resonances were observed. However, taking together the observation that certain ^{13}C resonances were unaffected (C_{1a}, C_{3a}, and C_3) while others (especially C_5, $C_{7'}$, and C_7) decreased in intensity or completely disappeared because of broadening, our experiments support the binding of lanthanides to PQQ in solution in the biologically relevant coordination pocket (site 1, Figure 2), as was also proposed for the uranyl ion by Peyton and co-workers.[47]

CONCLUSIONS

Although PQQ has been known and studied for over 50 years, many analytical details of species have been only sparingly reported and often relied on the use of the trimethyl ester. For the first time, we report full NMR, IR, and UV−vis characterization of PQQ and its water adduct. In addition, the interaction of PQQ in solution with biologically relevant metal ions (lanthanides and calcium) has been investigated, and these studies suggest that the coordination of lanthanides in nonaqueous solvents takes place in the biologically relevant pocket (site 1).[4,9] We further show that even if lanthanides have similar chemical properties, the subtle differences in ionic radii across the series impact the electronic structure as evidenced in the UV−vis spectrum of PQQ. These results will aid the development of PQQ-based model systems and further our understanding of lanthanide-dependent enzymes.

ASSOCIATED CONTENT

Supporting Information

The Supporting Information is available free of charge on the ACS Publications website at DOI: 10.1021/acs.inorgchem.9b00568.

NMR data for PQQ (ZIP)

NMR data for diamagnetic lanthanides (ZIP)

NMR data for paramagnetic lanthanides (ZIP)

Tables of NMR conditions and observed resonances, IR spectra and data, additional UV−vis spectra and data of PQQ in different solvents and with lanthanides, calculated ^{13}C NMR shifts of water adduct, mass spectrum of PQQ, TGA plots, and additional experimental procedures (PDF)

AUTHOR INFORMATION

Corresponding Author

*E-mail: lena.daumann@lmu.de.

ORCID

Lena J. Daumann: 0000-0003-2197-136X

Notes

The authors declare no competing financial interest.

ACKNOWLEDGMENTS

H.L. and L.J.D. gratefully acknowledge a Sachbeihilfe from the Deutsche Forschungsgemeinschaft (DFG) (project no. 392552271) and support from the Center for Integrated Protein Science Munich (CIPSM), SFB 749, and the LMU. We thank Dr. Jörg Stierstorfer for assistance with the TGA measurements.

DOI: 10.1021/acs.inorgchem.9b00568
Inorg. Chem. XXXX, XXX, XXX−XXX

REFERENCES

(1) Nomenclature Committee of the International Union of Biochemistry and Molecular Biology (NC-IUBMB). http://www.sbcs.qmul.ac.uk/iubmb/enzyme/EC1/ (visited Oct 16, 2018).

(2) Duine, J. A.; Frank, J.; Jongejan, J. A. Enzymology of Quinoproteins. *Advances in Enzymology and Related Areas of Molecular Biology*; John Wiley & Sons, Inc.: New York, 2006; pp 169−212.

(3) (a) Anthony, C.; Zatman, L. J. The Microbial Oxidation of Methanol. *Biochem. J.* **1964**, *92* (3), 609−614. (b) Anthony, C.; Zatman, L. J. The Microbial Oxidation of Methanol - 2. The methanol-oxidizing enzyme of *Pseudomonas* sp. M27. *Biochem. J.* **1964**, *92* (3), 614−621.

(4) Pol, A.; Barends, T. R. M.; Dietl, A.; Khadem, A. F.; Eygensteyn, J.; Jetten, M. S. M.; Op den Camp, H. J. M. Rare earth metals are essential for methanotrophic life in volcanic mudpots. *Environ. Microbiol.* **2014**, *16* (1), 255−264.

(5) Anthony, C. Quinoprotein-catalysed reactions. *Biochem. J.* **1996**, *320* (3), 697−711.

(6) Martinez-Gomez, N. C.; Vu, H. N.; Skovran, E. Lanthanide Chemistry: From Coordination in Chemical Complexes Shaping Our Technology to Coordination in Enzymes Shaping Bacterial Metabolism. *Inorg. Chem.* **2016**, *55* (20), 10083−10089.

(7) Semrau, J. D.; Di Spirito, A. A.; Gu, W.; Yoon, S., Metals and Methanotrophy. *Appl. Environ. Microbiol.* **2018**, *84* (6), DOI: 10.1128/AEM.02289-17.

(8) (a) Jahn, B.; Pol, A.; Lumpe, H.; Barends, T.; Dietl, A.; Hogendoorn, C.; Op den Camp, H.; Daumann, L. Similar but not the same: First Kinetic and Structural Analyses of a Methanol Dehydrogenase Containing a Europium Ion in the Active Site. *ChemBioChem* **2018**, *19*, 1147. (b) Good, N. M.; Vu, H. N.; Suriano, C. J.; Subuyuj, G. A.; Skovran, E.; Martinez-Gomez, N. C. Pyrroloquinoline Quinone Ethanol Dehydrogenase in Methylobacterium extorquens AM1 Extends Lanthanide-Dependent Metabolism to Multicarbon Substrates. *J. Bacteriol.* **2016**, *198* (22), 3109−3118. (c) Keltjens, J. T.; Pol, A.; Reimann, J.; Op den Camp, H. J. M. PQQ-dependent methanol dehydrogenases: rare-earth elements make a difference. *Appl. Microbiol. Biotechnol.* **2014**, *98* (14), 6163−6183.

(9) (a) Blake, C. C. F.; Ghosh, M.; Harlos, K.; Avezoux, A.; Anthony, C. The active site of methanol dehydrogenase contains a disulphide bridge between adjacent cysteine residues. *Nat. Struct. Mol. Biol.* **1994**, *1* (2), 102−105. (b) Williams, P. A.; Coates, L.; Mohammed, F.; Gill, R.; Erskine, P. T.; Coker, A.; Wood, S. P.; Anthony, C.; Cooper, J. B. The atomic resolution structure of methanol dehydrogenase from Methylobacterium extorquens. *Acta Crystallogr., Sect. D: Biol. Crystallogr.* **2005**, *61* (1), 75−79.

(10) (a) Chu, F.; Beck, D. A. C.; Lidstrom, M. E. MxaY regulates the lanthanide-mediated methanol dehydrogenase switch in Methylomicrobium buryatense. *PeerJ* **2016**, *4*, No. e2435. (b) Chu, F.; Lidstrom, M. E. XoxF Acts as the Predominant Methanol Dehydrogenase in the Type I Methanotroph *Methylomicrobium buryatense*. *J. Bacteriol.* **2016**, *198* (8), 1317−1325. (c) Good, N. M.; Walser, O. N.; Moore, R. S.; Suriano, C.; Huff, A. F.; Martinez-Gomez, N. C. Investigation of lanthanide-dependent methylotrophy uncovers complementary roles for alcohol dehydrogenase enzymes. *Bio Rxiv* **2018**, 329011. (d) Masuda, S.; Suzuki, Y.; Fujitani, Y.; Mitsui, R.; Nakagawa, T.; Shintani, M.; Tani, A. Lanthanide-Dependent Regulation of Methylotrophy in *Methylobacterium aquaticum* Strain 22A. *MSphere* **2018**, *3* (1), No. e00462-17. (e) Zheng, Y.; Huang, J.; Zhao, F.; Chistoserdova, L. Physiological Effect of XoxG(4) on Lanthanide-Dependent Methanotrophy. *mBio* **2018**, *9* (2), No. e02430-17.

(11) (a) Martinez-Gomez, N. C.; Skovran, E. In *Methane Biocatalysis: Paving the Way to Sustainability*. Kalyuzhnaya, M. G., Xing, X.-H., Eds.; Springer International Publishing: Basel, Switzerland, 2018. (b) Vu, H. N.; Subuyuj, G. A.; Vijayakumar, S.; Good, N. M.; Martinez-Gomez, N. C.; Skovran, E. Lanthanide-Dependent Regulation of Methanol Oxidation Systems in *Methylobacterium extorquens* AM1 and Their Contribution to Methanol Growth. *J. Bacteriol.* **2016**, *198* (8), 1250−1259.

(12) Bogart, J. A.; Lewis, A. J.; Schelter, E. J. DFT Study of the Active Site of the XoxF-Type Natural, Cerium-Dependent Methanol Dehydrogenase Enzyme. *Chem. - Eur. J.* **2015**, *21* (4), 1743−1748.

(13) (a) Lumpe, H.; Pol, A.; Op den Camp, H. J. M.; Daumann, L. J. Impact of the lanthanide contraction on the activity of a lanthanide-dependent methanol dehydrogenase - a kinetic and DFT study. *Dalton Trans.* **2018**, *47* (31), 10463−10472. (b) Wehrmann, M.; Billard, P.; Martin-Meriadec, A.; Zegeye, A.; Klebensberger, J., Functional Role of Lanthanides in Enzymatic Activity and Transcriptional Regulation of Pyrroloquinoline Quinone-Dependent Alcohol Dehydrogenases in Pseudomonas putida KT2440. *mBio* **2017**, *8* (3), DOI: 10.1128/mBio.00570-17. (c) Shiller, A. M.; Chan, E. W.; Joung, D. J.; Redmond, M. C.; Kessler, J. D. Light rare earth element depletion during Deepwater Horizon blowout methanotrophy. *Sci. Rep.* **2017**, *7*, 10389.

(14) Houck, D. R.; Hanners, J. L.; Unkefer, C. J.; van Kleef, M. A. G.; Duine, J. A. PQQ: Biosynthetic studies in Methylobacterium AM1 andHyphomicrobium X using specific ^{13}C labeling and NMR. *Antonie van Leeuwenhoek* **1989**, *56* (1), 93−101.

(15) Nakamura, N.; Kohzuma, T.; Kuma, H.; Suzuki, S. Synthetic and Structural Studies on Copper(II) Complexes Containing Coenzyme PQQ and Terpyridine. *Inorg. Chem.* **1994**, *33* (8), 1594−1599.

(16) Anthony, C.; Zatman, L. J. The microbial oxidation of methanol: The prosthetic group of the alcohol dehydrogenase of Pseudomonas sp. M27: a new oxidoreductase prosthetic group. *Biochem. J.* **1967**, *104* (3), 960−969.

(17) Westerling, J.; Frank, J.; Duine, J. A. The prosthetic group of methanol dehydrogenase from hyphomicrobium X: Electron spin resonance evidence for a quinone structure. *Biochem. Biophys. Res. Commun.* **1979**, *87* (3), 719−724.

(18) Salisbury, S. A.; Forrest, H. S.; Cruse, W. B. T.; Kennard, O. A novel coenzyme from bacterial primary alcohol dehydrogenases. *Nature* **1979**, *280*, 843.

(19) Duine, J. A.; Frank, J.; Verwiel, P. E. J. Structure and Activity of the Prosthetic Group of Methanol Dehydrogenase. *Eur. J. Biochem.* **1980**, *108* (1), 187−192.

(20) (a) Corey, E. J.; Tramontano, A. Total synthesis of the quinonoid alcohol dehydrogenase coenzyme (1) of methylotrophic bacteria. *J. Am. Chem. Soc.* **1981**, *103* (18), 5599−5600. (b) Jongejan, J. A.; Bezemer, R. P.; Duine, J. A. Synthesis of 13C- and 2H-labelled PQQ. *Tetrahedron Lett.* **1988**, *29* (30), 3709−3712. (c) Glinkerman, C. M.; Boger, D. L. Catalysis of Heterocyclic Azadiene Cycloaddition Reactions by Solvent Hydrogen Bonding: Concise Total Synthesis of Methoxatin. *J. Am. Chem. Soc.* **2016**, *138* (38), 12408−12413.

(21) Itoh, S.; Ogino, M.; Fukui, Y.; Murao, H.; Komatsu, M.; Ohshiro, Y.; Inoue, T.; Kai, Y.; Kasai, N. C-4 and C-5 adducts of cofactor PQQ (pyrroloquinolinequinone). Model studies directed toward the action of quinoprotein methanol dehydrogenase. *J. Am. Chem. Soc.* **1993**, *115* (22), 9960−9967.

(22) Itoh, S.; Kawakami, H.; Fukuzumi, S. Electrochemical Behavior and Characterization of Semiquinone Radical Anion Species of Coenzyme PQQ in Aprotic Organic Media. *J. Am. Chem. Soc.* **1998**, *120* (29), 7271−7277.

(23) Itoh, S.; Kawakami, H.; Fukuzumi, S. Model Studies on Calcium-Containing Quinoprotein Alcohol Dehydrogenases. Catalytic Role of Ca2+ for the Oxidation of Alcohols by Coenzyme PQQ (4,5-Dihydro-4,5-dioxo-1H-pyrrolo[2,3-f]quinoline-2,7,9-tricarboxylic Acid). *Biochemistry* **1998**, *37* (18), 6562−6571.

(24) (a) Jongejan, A.; Machado, S. S.; Jongejan, J. A. The enantioselectivity of quinohaemoprotein alcohol dehydrogenases: mechanistic and structural aspects. *J. Mol. Catal. B: Enzym.* **2000**, *8* (1), 121−163. (b) Duine, J. A. The PQQ story. *J. Biosci. Bioeng.* **1999**, *88* (3), 231−236.

(25) (a) Akagawa, M.; Nakano, M.; Ikemoto, K. Recent progress in studies on the health benefits of pyrroloquinoline quinone. *Biosci., Biotechnol., Biochem.* **2016**, *80* (1), 13−22. (b) Felton, L. M.; Anthony, C. Role of PQQ as a mammalian enzyme cofactor? *Nature* **2005**, *433*, E10.

DOI: 10.1021/acs.inorgchem.9b00568
Inorg. Chem. XXXX, XXX, XXX−XXX

(26) Wanner, M.; Sixt, T.; Klinkhammer, K.-W.; Kaim, W. First Experimental Structure of a 1:1 Metal Complex with a PQQ Cofactor Derivative outside Dehydrogenase Enzymes. *Inorg. Chem.* **1999**, *38* (11), 2753−2755.
(27) Mitome, H.; Ishizuka, T.; Shiota, Y.; Yoshizawa, K.; Kojima, T. Heteronuclear RuIIAgI Complexes Having a Pyrroloquinolinequinone Derivative as a Bridging Ligand. *Inorg. Chem.* **2013**, *52* (5), 2274−2276.
(28) Cotton, S. A.; Harrowfield, J. M. Lanthanides: Solvation. In *Encyclopedia of Inorganic and Bioinorganic Chemistry*; John Wiley & Sons, Ltd.: 2011.
(29) Frisch, M. J.; Trucks, G. W.; Schlegel, H. B.; Scuseria, G. E.; Robb, M. A.; Cheeseman, J. R.; Scalmani, G.; Barone, V.; Petersson, G. A.; Nakatsuji, H.; X. Li, M. C.; Marenich, A.; Bloino, J.; Janesko, B. G.; Gomperts, R.; Mennucci, B.; Hratchian, H. P.; Ortiz, J. V.; Izmaylov, A. F.; Sonnenberg, J. L.; Williams-Young, D.; Ding, F.; Lipparini, F.; Egidi, F.; Goings, J.; Peng, B.; Petrone, A.; Henderson, T.; Ranasinghe, D.; Zakrzewski, V. G.; Gao, J.; Rega, N.; Zheng, G.; Liang, W.; Hada, M.; Ehara, M.; Toyota, K.; Fukuda, R.; Hasegawa, J.; Ishida, M.; Nakajima, T.; Honda, Y.; Kitao, O.; Nakai, H.; Vreven, T.; Throssell, K.; Montgomery, J. A.; Jr, J. E. P.; Ogliaro, F.; Bearpark, M.; Heyd, J. J.; Brothers, E.; Kudin, K. N.; Staroverov, V. N.; Keith, T.; Kobayashi, R.; Normand, J.; Raghavachari, K.; Rendell, A.; Burant, J. C.; Iyengar, S. S.; Tomasi, J.; Cossi, M.; Millam, J. M.; Klene, M.; Adamo, C.; Cammi, R.; Ochterski, J. W.; Martin, R. L.; Morokuma, K.; Farkas, O.; Foresman, J. B.; Fox, D. J. *Gaussian 09*, Revision A.02; Gaussian, Inc.: Wallingford, CT, 2016.
(30) (a) Becke, A. D. Density-functional thermochemistry. III. The role of exact exchange. *J. Chem. Phys.* **1993**, *98* (7), 5648−5652. (b) Lee, C.; Yang, W.; Parr, R. G. Development of the Colle-Salvetti correlation-energy formula into a functional of the electron density. *Phys. Rev. B: Condens. Matter Mater. Phys.* **1988**, *37* (2), 785−789. (c) Petersson, G. A.; Al-Laham, M. A. A complete basis set model chemistry. II. Open-shell systems and the total energies of the first-row atoms. *J. Chem. Phys.* **1991**, *94* (9), 6081−6090. (d) Petersson, G. A.; Tensfeldt, T. G.; Montgomery, J. A. A complete basis set model chemistry. III. The complete basis set-quadratic configuration interaction family of methods. *J. Chem. Phys.* **1991**, *94* (9), 6091−6101. (e) Stephens, P. J.; Devlin, F. J.; Chabalowski, C. F.; Frisch, M. J. Ab Initio Calculation of Vibrational Absorption and Circular Dichroism Spectra Using Density Functional Force Fields. *J. Phys. Chem.* **1994**, *98* (45), 11623−11627. (f) Vosko, S. H.; Wilk, L.; Nusair, M. Accurate spin-dependent electron liquid correlation energies for local spin density calculations: a critical analysis. *Can. J. Phys.* **1980**, *58* (8), 1200−1211.
(31) (a) Barone, V.; Cossi, M. Quantum Calculation of Molecular Energies and Energy Gradients in Solution by a Conductor Solvent Model. *J. Phys. Chem. A* **1998**, *102* (11), 1995−2001. (b) Cossi, M.; Rega, N.; Scalmani, G.; Barone, V. Energies, structures, and electronic properties of molecules in solution with the C-PCM solvation model. *J. Comput. Chem.* **2003**, *24* (6), 669−681.
(32) (a) Cheeseman, J. R.; Trucks, G. W.; Keith, T. A.; Frisch, M. J. A comparison of models for calculating nuclear magnetic resonance shielding tensors. *J. Chem. Phys.* **1996**, *104* (14), 5497−5509. (b) Wolinski, K.; Hinton, J. F.; Pulay, P. Efficient implementation of the gauge-independent atomic orbital method for NMR chemical shift calculations. *J. Am. Chem. Soc.* **1990**, *112* (23), 8251−8260.
(33) Ikemoto, K.; Mori, S.; Mukai, K. Synthesis and crystal structure of pyrroloquinoline quinol (PQQH2) and pyrroloquinoline quinone (PQQ). *Acta Crystallogr., Sect. B: Struct. Sci., Cryst. Eng. Mater.* **2017**, *73* (3), 489−497.
(34) (a) Kano, K.; Mori, K.; Uno, B.; Kubota, T.; Ikeda, T.; Senda, M. Voltammetric determination of acid dissociation constants of pyrroloquinoline quinone and its reduced form under acidic conditions. *Bioelectrochem. Bioenerg.* **1990**, *24* (2), 193−201. (b) Kano, K.; Mori, K.; Uno, B.; Kubota, T.; Ikeda, T.; Senda, M. Voltammetric and spectroscopic studies of pyrroloquinoline quinone coenzyme under neutral and basic conditions. *Bioelectrochem. Bioenerg.* **1990**, *23* (3), 227−238. (c) Zhang, Z. P.; Tillekeratne, L. M. V.; Kirchhoff, J. R.; Hudson, R. A. High-Performance Liquid Chromatographic Separation and pH-Dependent Electrochemical Properties of Pyrroloquinoline Quinone and Three Closely Related Isomeric Analogues. *Biochem. Biophys. Res. Commun.* **1995**, *212* (1), 41−47.
(35) (a) Duine, J. A.; Frank, J.; Verwiel, P. E. J. Characterization of the Second Prosthetic Group in Methanol Dehydrogenase from *Hyphomicrobium* X. *Eur. J. Biochem.* **1981**, *118* (2), 395−399. (b) Dekker, R. H.; Duine, J. A.; Frank, J.; Verwiel, P. E. J.; Westerling, J. Covalent Addition of H2O, Enzyme Substrates and Activators to Pyrrolo-quinoline Quinone, the Coenzyme of Quinoproteins. *Eur. J. Biochem.* **1982**, *125* (1), 69−73.
(36) Zheng, Y.-J.; Bruice, T. C. Conformation of coenzyme pyrroloquinoline quinone and role of Ca(2+) in the catalytic mechanism of quinoprotein methanol dehydrogenase. *Proc. Natl. Acad. Sci. U. S. A.* **1997**, *94* (22), 11881−11886.
(37) (a) GRAS Exemption Claim for Pyrroloquinoline Quinone (PQQ) Disodium Salt Zhejiang Hisun Pharmaceutical Co. Ltd.: https://www.fda.gov/downloads/Food/IngredientsPackagingLabeling/GRAS/NoticeInventory/ucm508141.pdf (visited Jan 11th 2019), 2016. (b) Nakamoto, K. *Infrared and Raman Spectra of Inorganic and Coordination Compounds, Part B: Applications in Coordination, Organometallic, and Bioinorganic Chemistry*, 6th ed.; John Wiley & Sons, Inc.: 2009; Chapter 1.
(38) Dimitrijevic, N. M.; Poluektov, O. G.; Saponjic, Z. V.; Rajh, T. Complex and Charge Transfer between TiO2 and Pyrroloquinoline Quinone. *J. Phys. Chem. B* **2006**, *110* (50), 25392−25398.
(39) Tommasi, L.; Shechter-Barloy, L.; Varech, D.; Battioni, J. P.; Donnadieu, B.; Verelst, M.; Bousseksou, A.; Mansuy, D.; Tuchagues, J. P. Synthesis of Pyrroloquinolinequinone Analogs. Molecular Structure and Moessbauer and Magnetic Properties of Their Iron Complexes. *Inorg. Chem.* **1995**, *34* (6), 1514−1523.
(40) Renny, J. S.; Tomasevich, L. L.; Tallmadge, E. H.; Collum, D. B. Method of continuous variations: applications of job plots to the study of molecular associations in organometallic chemistry. *Angew. Chem., Int. Ed.* **2013**, *52* (46), 11998−12013.
(41) Noar, J. B.; Rodriguez, E. J.; Bruice, T. C. Synthesis of 9-decarboxymethoxatin. Metal complexation of methoxatin as a possible requirement for its biological activity. *J. Am. Chem. Soc.* **1985**, *107* (24), 7198−7199.
(42) Suzuki, S.; Sakurai, T.; Itoh, S.; Ohshiro, Y. Preparation and characterization of ternary copper(II) complexes containing coenzyme PQQ and bipyridine or terpyridine. *Inorg. Chem.* **1988**, *27* (4), 591−592.
(43) Nakamura, N.; Kohzuma, T.; Kuma, H.; Suzuki, S. Synthetic and structural studies on copper (II) complexes containing coenzyme PQQ and terpyridine. *Inorg. Chem.* **1994**, *33*, 1594.
(44) Schwederski, B.; Kasack, V.; Kaim, W.; Roth, E.; Jordanov, J. Ambidentes Verhalten des "neuen Vitamins" Methoxatin (Cofaktor PQQ) gegenüber Metallen: Koordinative Stabilisierung der Pyrrolid- und der Semichinon-Form. *Angew. Chem.* **1990**, *102* (1), 74−76.
(45) Ishida, T.; Doi, M.; Tomita, K.; Hayashi, H.; Inoue, M.; Urakami, T. Molecular and crystal structure of PQQ (methoxatin), a novel coenzyme of quinoproteins: extensive stacking character and metal ion interaction. *J. Am. Chem. Soc.* **1989**, *111* (17), 6822−6828.
(46) Itoh, S.; Kawakami, H.; Fukuzumi, S. Modeling of the Chemistry of Quinoprotein Methanol Dehydrogenase. Oxidation of Methanol by Calcium Complex of Coenzyme PQQ via Addition-Elimination Mechanism. *J. Am. Chem. Soc.* **1997**, *119* (2), 439−440.
(47) VanEngelen, M. R.; Szilagyi, R. K.; Gerlach, R.; Lee, B. D.; Apel, W. A.; Peyton, B. M. Uranium exerts acute toxicity by binding to pyrroloquinoline quinone cofactor. *Environ. Sci. Technol.* **2011**, *45* (3), 937−942.
(48) McSkimming, A.; Cheisson, T.; Carroll, P. J.; Schelter, E. J. Functional Synthetic Model for the Lanthanide-Dependent Quinoid Alcohol Dehydrogenase Active Site. *J. Am. Chem. Soc.* **2018**, *140* (4), 1223−1226.
(49) Cotton, S. A.; Harrowfield, J. M. Lanthanides: Coordination Chemistry. *Encyclopedia of Inorganic and Bioinorganic Chemistry*; John Wiley & Sons, Ltd: 2011.

DOI: 10.1021/acs.inorgchem.9b00568
Inorg. Chem. XXXX, XXX, XXX−XXX

(50) Job, P. Formation and Stability of Inorganic Complexes in Solution. *Annali di Chimica Applicata* **1928**, *9*, 113−203.
(51) (a) Henrie, D. E.; Fellows, R. L.; Choppin, G. R. Hypersensitivity in the electronic transitions of lanthanide and actinide complexes. *Coord. Chem. Rev.* **1976**, *18* (2), 199−224. (b) Karraker, D. G. Hypersensitive transitions of six-, seven-, and eight-coordinate neodymium, holmium, and erbium chelates. *Inorg. Chem.* **1967**, *6* (10), 1863−1868.
(52) Ouali, N.; Bocquet, B.; Rigault, S.; Morgantini, P.-Y.; Weber, J.; Piguet, C. Analysis of Paramagnetic NMR Spectra of Triple-Helical Lanthanide Complexes with 2,6-Dipicolinic Acid Revisited: A New Assignment of Structural Changes and Crystal-Field Effects 25 Years Later. *Inorg. Chem.* **2002**, *41* (6), 1436−1445.
(53) (a) Vonci, M.; Mason, K.; Suturina, E. A.; Frawley, A. T.; Worswick, S. G.; Kuprov, I.; Parker, D.; McInnes, E. J. L.; Chilton, N. F. Rationalization of Anomalous Pseudocontact Shifts and Their Solvent Dependence in a Series of C3-Symmetric Lanthanide Complexes. *J. Am. Chem. Soc.* **2017**, *139* (40), 14166−14172. (b) Poh, A. W. J.; Aguilar, J. A.; Kenwright, A. M.; Mason, K.; Parker, D. Aggregation of Rare Earth Coordination Complexes in Solution Studied by Paramagnetic and DOSY NMR. *Chem. - Eur. J.* **2018**, *24* (60), 16170−16175. (c) Suturina, E. A.; Mason, K.; Geraldes, C. F. G. C.; Kuprov, I.; Parker, D. Beyond Bleaney's Theory: Experimental and Theoretical Analysis of Periodic Trends in Lanthanide-Induced Chemical Shift. *Angew. Chem., Int. Ed.* **2017**, *56* (40), 12215−12218.
(54) Blackburn, O. A.; Edkins, R. M.; Faulkner, S.; Kenwright, A. M.; Parker, D.; Rogers, N. J.; Shuvaev, S. Electromagnetic susceptibility anisotropy and its importance for paramagnetic NMR and optical spectroscopy in lanthanide coordination chemistry. *Dalton Trans.* **2016**, *45* (16), 6782−6800.
(55) (a) McConnell, H. M.; Robertson, R. E. Isotropic Nuclear Resonance Shifts. *J. Chem. Phys.* **1958**, *29* (6), 1361−1365. (b) Bleaney, B. Nuclear magnetic resonance shifts in solution due to lanthanide ions. *J. Magn. Reson.* **1972**, *8* (1), 91−100.

DOI: 10.1021/acs.inorgchem.9b00568
Inorg. Chem. XXXX, XXX, XXX−XXX